

MITIGATION OF TACAN/DME INTERFERENCES FOR L5/E5 SPACE-BORNE GNSS RECEIVERS IN LEO. FIRST SIMULATION RESULTS WITH FOCUS ON RADIO-OCCULTATION MISSIONS

NAVITEC 2022

05 - 07 April 2022

ESA/ESTEC, Noordwijk, The Netherlands

Laurent Lestarquit⁽¹⁾, Christelle Dulery⁽¹⁾, Raoul Prévost⁽²⁾, Mariano Iervolino⁽³⁾

⁽¹⁾CNES

18 Avenue Edouard Belin

31401 Toulouse Cedex, France

Email: laurent.lestarquit@cnes.fr, christelle.dulery@cnes.fr

⁽²⁾TESA

7 Boulevard de la gare

31500 Toulouse, France

Email: raoul.prevost@tesa.prd.fr

⁽³⁾Agenium

1 Avenue de l'Europe

31400 Toulouse, France

Email: mariano.iervolino@agenium.com

ABSTRACT

At their design time, GPS L5 and GALILEO E5a/E5b signals compatibility with TACAN/DME was studied for aeronautical users with altitude limited up to 40,000 feet, but not for space-borne users. Aircraft would see a few strong pulses and a mitigation technique as simple as pulse blanking would usually work as mitigation means.

For space-borne GNSS receivers in Low Earth Orbit (LEO), if the larger free space losses lead to weaker received TACAN/DME signals, the number of beacons in visibility is much higher, reaching in the worst locations a total over two hundred with more than half of them having a peak power above or close to the noise floor, making time blanking a poor mitigation means. Therefore, other mitigation techniques performances need to be assessed in order to determine which techniques are best suited.

A simulation tool was developed to compute the post correlation C/N_0 degradation due to TACAN/DME on a LEO with and without mitigation means enabled. The equivalent post-correlation noise (N_0) increase due to TACAN/DME, or what remains after a mitigation technique is applied, is simulated using the Spectral Separation Coefficient (SSC) methodology to emulate the effect of GNSS signal de-spreading in the receiver correlation process. The part of the useful signal carrier suppressed by the application of a mitigation technique (time blanking and/or frequency notch filtering) is taken into account in the simulation.

This study is focusing on radio-occultation (RO) missions which are the more sensitive to TACAN/DME interferences. Indeed, a medium-gain antenna (9–18 dB typical) is steered toward the earth limb resulting in having many TACAN/DME transmitters inside its main lobe. This configuration can lead to a high received power from them, as the LEO RO satellite is also in their main antenna lobe. In this configuration, the C/N_0 degradation, plotted on a geographic map can reach up to 13.8 dB in the absence of mitigation over the European TACAN/DME hotspot.

Several promising mitigation techniques have been included in the simulation tool to determine which one shall be implemented on board a LEO RO satellite mission: time domain pulse blanking, Frequency Domain Adaptive Filtering (FDAF) or hybrid blanking.

We also considered implementing pulse cancellation, an attractive technique in theory, but not so in practice due to the deviation of the actual transmitted signals with respect to their theoretical models.

As anticipated, pulse blanking does not perform well at the LEO orbit. It can be actually worse than doing nothing when there is a large number of TACAN/DME transmitters in visibility since it leads to a high loss in useful GNSS signals during the blanking process.

As detailed in this paper, hybrid time domain and frequency domain methods are more effective when frequency notch filtering is applied over a limited time window. For FDAF, windows have fixed boundaries, independently of the

presence of interfering pulses, whereas in the hybrid method, the time windows are centered on the detected pulses. The FDAF method reduced the peak interference down to 5.6 dB. The hybrid blanking method has the best performances with a worst degradation which can be reduced to 4.3 dB over the European hotspot.

INTRODUCTION

GPS L5 and GALILEO E5a/E5b signals share an aeronautical band with the return link of several channels of TACAN/DME which are ground beacons transmitting powerful pulsed signal with a shaped antenna pattern with maximum EIRP (Equivalent Isotropic Radiated Power) located a few degrees of elevation above the horizon. When these GNSS signals were designed, compatibility was studied only for aeronautical users with altitude limited up to 40,000 feet [1, 2]. An aircraft would usually see up to a dozen high power signals from TACAN/DME transmitters in the GNSS band. Pulse blanking would then work efficiently as mitigation means. Since the design of these GNSS signals, many improved mitigation techniques have been proposed and studied in an airborne context: Frequency Domain Adaptive Filtering (FDAF) [3], Frequency notch filtering [4], Hybrid blanking [4], wavelets processing [5], pulse cancellation [6].

In the case of space-borne applications, very little has been published. The literature is limited to the application of pulse blanking applied to a large number of received TACAN/DME in-visibility [7] and to a mitigation technique specific to Interferometric GNSS Reflectometry applications [8].

For LEO (Low Earth Orbit) applications, the problem is that even though free space losses lead to much weaker received TACAN/DME signals than for airborne applications. Also, since the number of beacons in visibility with a peak power above the noise floor is significantly higher, up to more than 200 beacons over the European hotspot, time blanking is a poor mitigation approach because a larger number of beacons lead to a higher blanking fraction of the total useful GNSS signal as well. Therefore, in this paper, we explore other mitigation techniques in order to determine which techniques shall be used for space-borne applications.

USEFUL TACAN/DME CHARACTERISTICS

The typical signal peak maximum EIRP is usually around 37 dBW for DME and 40 dBW for TACAN. Fortunately, both are transmitting short pairs of pulse separated by 12 μs with each pulse having an equivalent peak power transmission length of 2.64 μs . TACAN can also transmit sequences of 12 consecutive pulses. Ideal TACAN/DME pulses envelope are usually modeled according to (1) where $\alpha = 4.5 \cdot 10^{11} \text{ s}^{-2}$, and $\Delta t = 12 \mu\text{s}$.

$$s(t) = e^{-\frac{\alpha}{2}\left(t-\frac{\Delta t}{2}\right)^2} + e^{-\frac{\alpha}{2}\left(t+\frac{\Delta t}{2}\right)^2} \quad (1)$$

The resulting pulse model is in Figure 1. The double pulse per second (dpps) rate is dependent upon interrogations by air traffic and has a maximum of 2,700 double pulses per second for DME and 3,600 pulses for TACAN [1]. These maximum rates can be effectively achieved in case of heavy air traffic, for this reason, they will be used throughout this article. Even in case no air traffic is present, TACAN and DME transmit at a residual pulse rate in the order of 1,350 dpps. At maximum pulse rate, this leads to an average to peak power ratio of $2.64 \cdot 10^{-6} \cdot 2700 \cdot 2 = 0.0143$, meaning the mean transmitted EIRP is attenuated by 18.4 dB down to a mean power maximum EIRP of rather 18.6 dBW (21.6 dBW) for DME (TACAN). Pulses have a half-amplitude length of 3.5 μs . TACAN/DME channels are 1 MHz apart, ranging from 960 to 1213 MHz with the channels above 1165 MHz falling inside the GNSS bands. The jammer ideal PSD for a double pulse is in Figure 2.

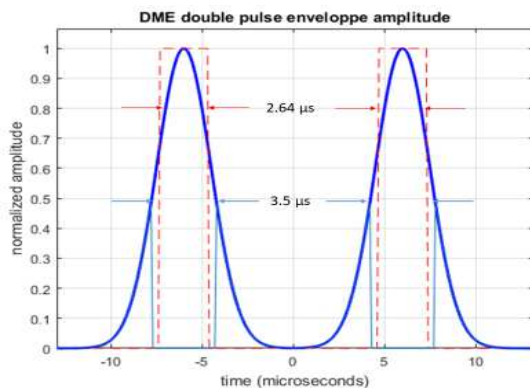


Figure 1: Ideal TACAN/DME double pulse envelope

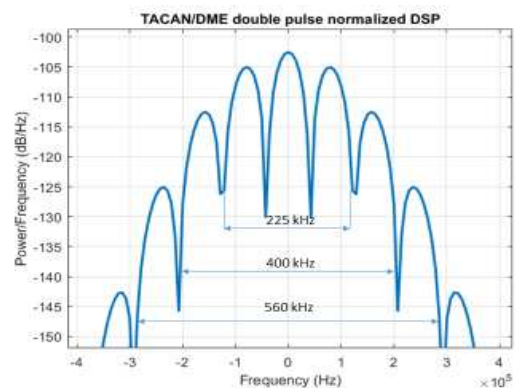


Figure 2 TACAN/DME theoretical normalized PSD

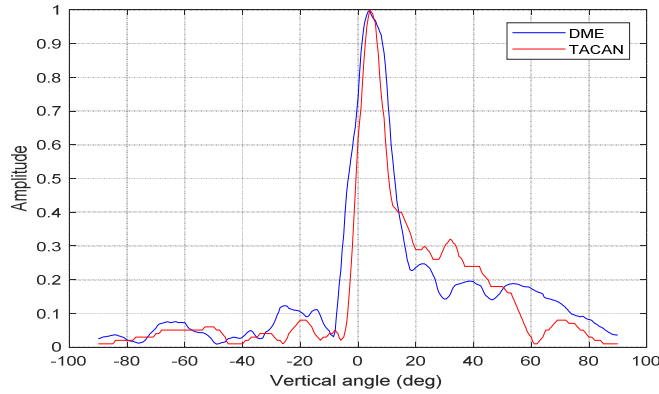


Figure 3: Typical DME/TACAN normalized antenna pattern

DME ANTENNA PATTERN CHARACTERISTICS

There exist several types of transmit antenna patterns for DME, with various maximum gain at diverse elevations (2° , 4° , 7° and 10°). We could not find any information about which antenna pattern to map to which DME in existing DME database. This is an open point to ensure accurate modelling because the antenna pattern shape has a significant impact on the link budget. Without this knowledge, for our simulation we chose to use the typical DME/TACAN antenna normalized pattern (Figure 3) defined in [12].

LINK BUDGET FOR LEO USE CASES.

A link budget assuming an isotropic 0 dB gain receiving antenna was developed in [7]. We improved this link budget considering receiving antenna patterns for 3 types of missions: (a) Precise Orbit Determination using a hemispherical zenith pointing antenna, (b) POD using 2 coupled hemispherical antennas pointed in opposite directions toward the front and rear of the satellite (as it was the case in the Microscope mission), and (c) Radio-occultation mission with an 11 dB gain antenna pointing toward the earth limb, tilted 20° below the horizon, as shown in Figure 4.

The link budgets were considered for the simple canonical case in which the spacecraft is flying directly overhead a single DME, passing exactly at its zenith, in order to grasp the order of magnitude of the interferences. In this article only the radio-occultation scenario will be presented, indeed it is the most unfavorable scenario as there exist links with both transmit and receive antenna gain close to their maximum.

Throughout the article, the considered satellite is a LEO flying at 500 km altitude in a 95° inclined sun-synchronous orbit. Its RO antennas have a maximum gain of 11 dB. There are two antennas, pointed 20° below the local horizontal plane, one toward the satellite velocity direction for setting occultations and one toward the anti-velocity direction for rising occultation. Each antenna is connected to its own RF front-end therefore they are independent with respect to interferences computations. In the simulation results, only the fore antenna on northbound tracks will be considered.

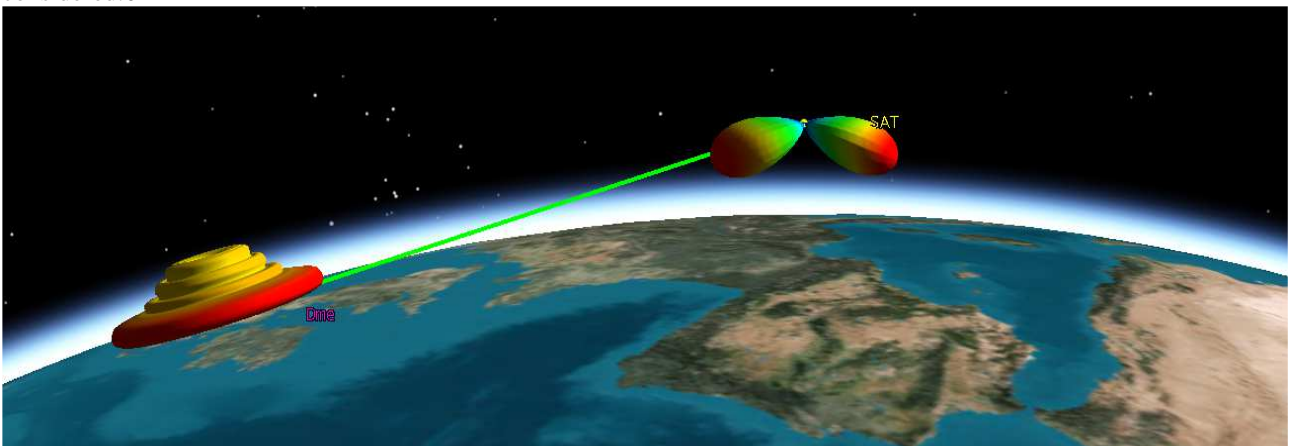


Figure 4: GNSS Radio-Occultation typical jamming configuration with DME transmit and RO receive antenna gain patterns, and a link passing through both antenna main lobes.

SSC METHODOLOGY

The methodology used to compute the degradation on the GNSS signal is known as SSC (Spectral Separation Coefficient) methodology. The C/N_0 effective degradation is computed after the correlation process has taken place in the GNSS receiver. Therefore it emulates the effect of GNSS signal de-spreading in the signal processing. This methodology has been widely used for GNSS interference computations, including during the GALILEO signal design phase. References about this method can be found in [10] and [11].

There are two mechanisms that lead to C/N_0 degradation in the presence of a jammer:

- Increase of post-correlation effective Noise (N_{eff}) due to a jammer, or what remains after a mitigation method is applied to filter out the jammer impact.
- Reduction of the desired signal useful carrier power to noise ratio, essentially due to blanking or filtering of the desired signal and noise in the process of mitigating the jammer, is a collateral effect of jamming mitigation.

The C/N_0 degradation due to the combination of both mechanisms is:

$$\text{deg} \left(\frac{C}{N_0} \right) = \frac{1 + \sum_i J_i \times SSC_i(\Delta f_i)}{DSCNR} \quad (2)$$

where $\text{deg} \left(\frac{C}{N_0} \right)$ is the effective C/N_0 degradation relative to the unjammed C/N_0 . J_i is the i^{th} jammers mean power received at the input of the GNSS receiver signal processing channels, or whatever remains of it after a mitigation method has been applied, $SSC_i(\Delta f_i)$ is the Spectral Separation Coefficient between the desired GNSS signal and the i^{th} jammer whose center frequency is offset by Δf_i from the GNSS carrier frequency, and $DSCNR$ is the ‘‘Desired Signal Carrier to Noise Ratio Reduction’’ remaining at the input of the receiver processing channels after a jammer mitigation method has been applied.

Note that (2) has to be computed using linear units (no log-scale dB units, appropriate conversions have to be made).

The convention used throughout this article is $\text{deg} \left(\frac{C}{N_0} \right)$ is a degradation; therefore it is positive when expressed in dB.

The SSC is computed using the standard SSC equation:

$$SSC_i(\Delta f_i) = \int_{-\beta_r/2}^{\beta_r/2} G_{GNSS}(f) \cdot G_{J_i}(f - \Delta f_i) \cdot |H(f)|^2 df \quad (3)$$

where β_r is the GNSS front-end bandwidth, $G_{GNSS}(f)$ is the Power Spectral Density (PSD) of the desired GNSS signal normalized to unity, G_{J_i} is the jammer PSD normalized to unity, or its residual PSD after a mitigation method is applied, $H(f)$ is the receiver front-end filter, for simplicity we used a brick wall filter of bandwidth β , therefore the expression used in the end is:

$$SSC_i(\Delta f_i) = \int_{-\beta_r/2}^{\beta_r/2} G_{GNSS}(f) \cdot G_{J_i}(f - \Delta f_i) df \quad (4)$$

NARROW BAND JAMMER APPROXIMATION

Compared to a BPSK(10) GNSS signal that has a 20.46 MHz wide main lobe, the jamming signal has a much narrower band: 99.5 % of its power is concentrated in its centre 400 kHz, therefore the narrowband approximation for the computation of SSC works well enough, except when the GNSS DSP changes rapidly, that is in the knoll of the GNSS DSP. Fortunately, when this happens, the induced jamming is highly reduced anyway and insignificant. Therefore, the SSC can be approximated to within 0.1 dB with the following formula:

$$SSC_i(\Delta f_i) \cong G_{GNSS}(\Delta f_i) \quad (5)$$

This approximation makes much easier to handle the effect of a jammer residual after a mitigation method is applied. Indeed, we supposed the SSC of the residual jammer does not change significantly after the anti-jamming method has been applied, all that needs to be taken into account is the total power reduction of the jammer by the method, from time blanking and/or frequency filtering.

UNITARY DEGRADATION WITHOUT MITIGATION METHODS FOR THE DIVERSE MISSIONS

Without applied mitigation method, the useful GNSS signal is not reduced ($DSCNR = 1$) and (2) simplifies to:

$$deg\left(\frac{C}{N_0}\right) = 1 + \sum_i \frac{J_i}{N_0} \times SSC_i(\Delta f_i) \quad (6)$$

The C/N_0 degradation corresponding to the link budget computed in Figure 5 with a noise floor spectral density of $N_0 = -201.5$ dBW/Hz (this value will be used throughout the article) are given in the Figure 6 for a DME in case of a maximum SSC of -70.1 dBHz⁻¹ (corresponding to a DME frequency of 1176 or 1177 MHz).

TACAN/DME DEGRADATION SIMULATION

To compute the degradation due to the many TACAN/DME in visibility, a simulator based on the SSC methodology was developed and a TACAN/DME database was used for simulations over the European hotspot. This simulator computes the link budget with every beacon and the aggregate C/N_0 degradation according to (2).

Without any mitigation method applied, the resulting C/N_0 degradation map over the European hotspot is given in Figure 8, for the forward-looking antenna on the ascending track of a 500 km high, 95° inclined polar orbit. The worst degradation is 13.8 dB and occurs when the satellite is located at 32°N, 14°E, quite a significant degradation that would impair the use of L5/E5a for RO.

PULSE TIME BLANKING

The simplest mitigation method, pulse blanking was applied to a full-time window of width d_M centered on every single pulse that is detected, as described in [4]. This is the correct implementation of time blanking. There exists another implementation in which only the digitized signal over a given threshold is blanked, but this implementation leads to keeping signal fragments in the middle of a pulse, with the slope of the remaining signal driven mostly by the interfering

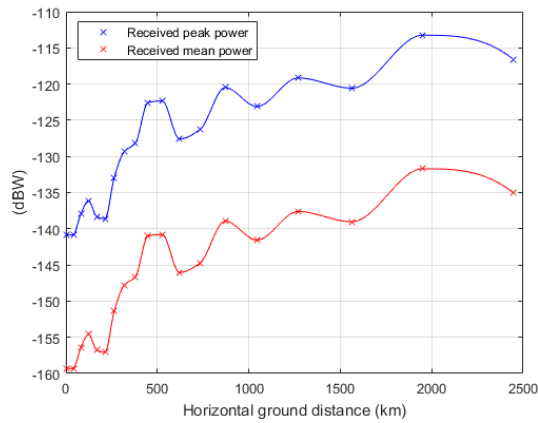


Figure 5: Link budget for a LEO RO satellite flying straight over a DME

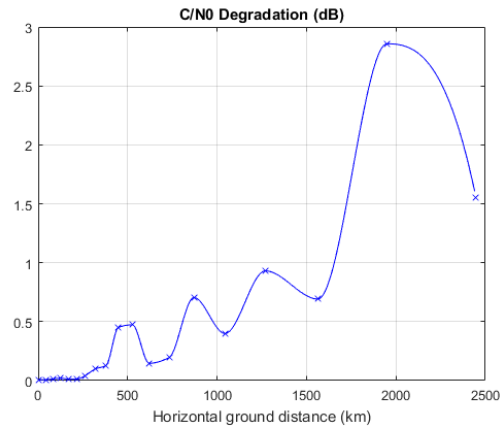


Figure 6: C/N_0 degradation for a LEO RO satellite flying straight over a DME (for $SSC = -70.1$ dBHz⁻¹)

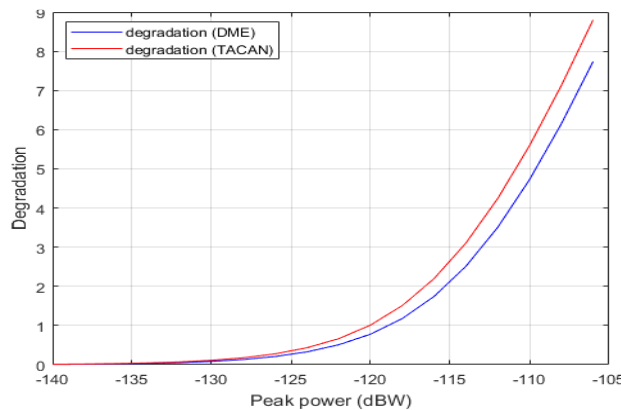


Figure 7: Degradation according to the received peak power, for TACAN and DME operation at maximum pulse rate, for a maximum SSC of -70.1 dB/Hz.

pulse. It is nonsense not to remove such a corrupted signal, and moreover, it is the envelope of the complex digitized I&Q signal that shall be taken into account.

In our simulation, we used $d_M = 5.5 \mu s$, which leads to blanking 99.0% of each pulse power. We chose the blanking window as short as possible in order not to lose too much useful GNSS signal power, indeed the reduction of the useful signal power according to the blanking duty cycle (Bdc) is given by:

$$DSCNR = 1 - Bdc = e^{-P_{FA} f_s d_M} \prod_i (1 - P_{Di} f_{pi} d_M) \quad (7)$$

where P_{Di} is the probability of detection of pulses originating from the i^{th} jammer, f_{pi} is the frequency of single pulses, that is 2·2700 for DME, 2·3600 for TACAN. P_{FA} is the probability of false alarm, f_s is the signal sampling frequency. In time domain, if the amplitude A of the incoming signal relative to the complex noise floor variance σ exceeds the threshold corresponding to the P_{FA} according to (8), a pulse is detected and blanked. In our simulation, we used $P_{FA} = 10^{-6}$ and $f_s = 24$ MSamples/s, the probability of detection according to the A/σ ratio is plotted in Figure 13.

$$A/\sigma > Threshold = \sqrt{-\ln(P_{FA})} \quad (8)$$

Considering a receiver with a minimum RF bandwidth of 20.46 MHz, the total noise power is equal to -128.5 dBW, therefore Figure 13 tells that most of the pulse with peak power above -119,5 dBW will be detected, almost none with power below -126,5 dBW, and with a transition zone in between.

At the worst locations (32°N and 14°E), the peak received power distribution (Figure 12) shows that 85 transmitters have a peak power > -120 dBW and were completely blanked with an additional 42 transmitters that were partially blanked. This high number leads to a higher useful GNSS signal suppression and explains the poor results obtained in Figure 9, infact when many transmitters are present, the degradation is worse, up to 17.6 dB.

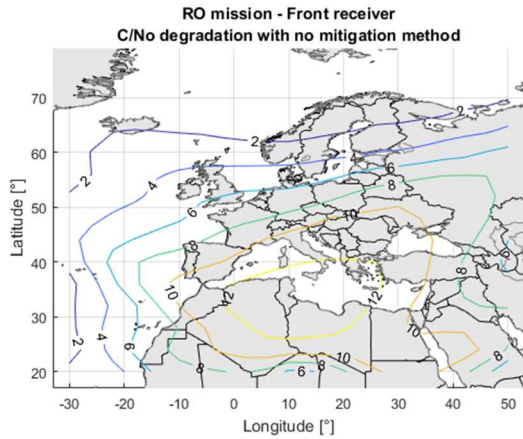


Figure 8: C/N0 degradation with no mitigation method.

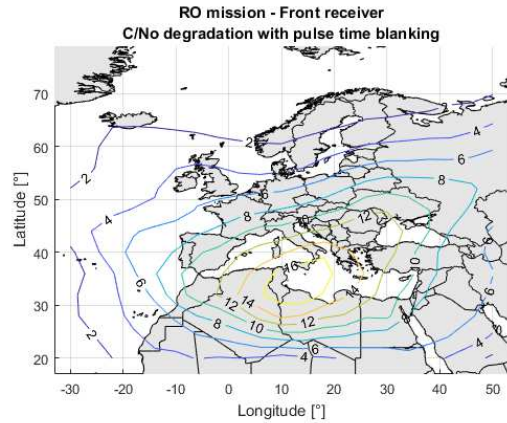


Figure 9: C/N0 degradation with pulse time blanking.

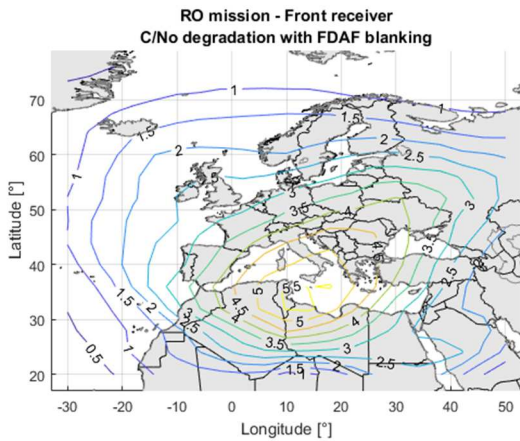


Figure 10: C/N0 degradation with FDAF blanking.

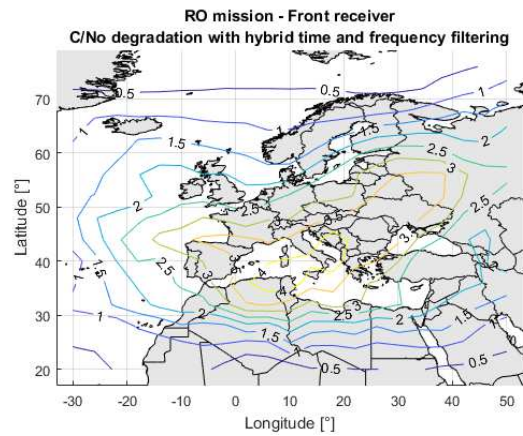


Figure 11: C/N0 degradation with hybrid blanking

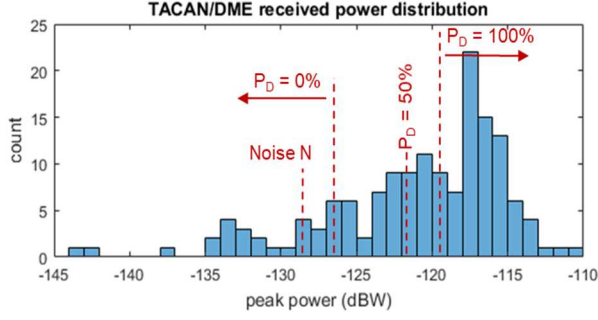


Figure 12: Distribution of received DME pulse peak power at worst location (32°N, 14°E)

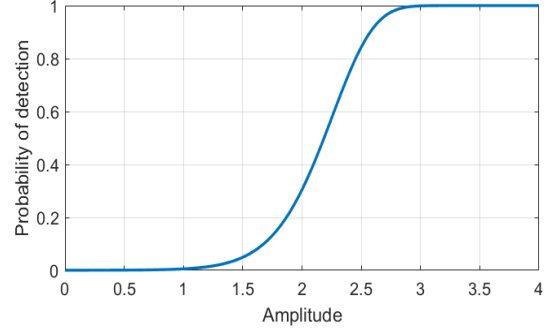


Figure 13: Single pulse P_D as a function of peak amplitude to noise (C/N) ratio for $P_{FA}=10^{-6}$

FDAF (FREQUENCY DOMAIN ADAPTIVE FILTERING)

This is a hybrid time domain and frequency domain method described in [3]. In the time domain, the signal is divided in fixed-length windows over which a Fast Fourier Transform (FFT) is applied. In the presence of white noise only, the FFT shall be flat, a threshold is determined with a given false alarm rate. If certain points of the incoming signal's FFT exceed that threshold, they are considered corrupted by interference and set to zero, and finally the inverse FFT is performed to obtain the signal back in the time domain with the detected interferences removed. The modelisation of the fraction of jammer and useful signal removed were implemented in the simulator.

As the time windows have fixed lengths and boundaries, a pulse can straddle over a time window boundary, which might impair somewhat the efficiency of the method to remove the interference.

In the simulation, a fixed length window of 256 points was used, with a sampling frequency of 24 MHz, that is a window length of 10.67 μ s. Results are presented in Figure 10. The C/N_0 degradation at worst location has been reduced from 13.8 dB to 5.6 dB

HYBRID BLANKING

This is another time domain and frequency domain method described in [4]. In the time domain, when an interference pulse is detected, its frequency is determined in the frequency domain, and the notch filtering of frequency width b_M of a slice of time length d_M centered on the pulse is applied. We used $d_M = 8 \mu$ s, and $b_M = 540$ kHz, a time and frequency window in which 99.96% of a pulse power is located

The reduction in useful signal power is given by:

$$DSCNR = e^{-2P_{FA}f_c d_M b_M / B} \prod_i (1 - P_{D_i} f_{p_i} d_M R b_M(\Delta f_i) b_M / B) \quad (10)$$

where B is the useful signal total bandwidth, and $R b_M(\Delta f_i)$ is a weighting factor linked to the useful signal PSD band that is cut by the notch filtering:

$$R b_M(\Delta f_i) = \frac{B}{b_M} \frac{\int_{\Delta f_i - b_M/2}^{\Delta f_i + b_M/2} \text{PSD}_{\text{GNSS}}(f) df}{\int_{-B/2}^{B/2} \text{PSD}_{\text{GNSS}}(f) df} \quad (11)$$

Results are presented in Figure 11. The C/N_0 degradation at worst location has been reduced from 13.8 dB to 4.3 dB, that is better than the FDAF method. Most of the residual degradation is due to un-detected pulses. The worst degradation occurs at 36°N, 10°W due to more undetected TACAN/DME present at this location.

PULSE CANCELLATION

Pulse cancellation is in theory the most attractive TACAN/DME interference technique. Indeed, as the expected pulse shape is defined in (1), it is possible to estimate, for each detected pulse, its amplitude, delay and carrier phase, in order to subtract a reconstructed pulse from the desired signal. If these parameters are well estimated, it would almost completely remove the interfering pulse, leaving the desired signal unimpaired.

However, in practice, field measurement of several TACAN/DME beacons shows that there is a significant deviation between (1) and the actual transmitted pulses. Figure 14 shows an example in which the transmitted pulse envelope differs significantly from the model. In addition, the phase linearity of the real-world signal is poor, leading to

a residual signal that is significant throughout each pulse. In the given example, the residual jammer power would be 7.32% (or -11.3 dB) after cancellation, making this method less attractive than expected. In addition, field measurement showed that each TACAN/DME seems to have its own unique signature, and this method was not further studied.

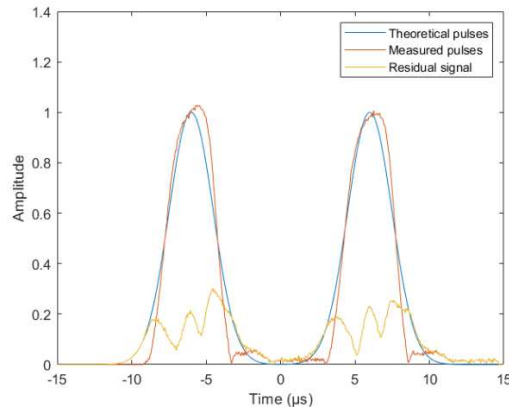


Figure 14: Deviation of an observed DME pulse in Toulouse and the theoretical pulse

CONCLUSION

The simulation shows that for space-borne applications the impact of jamming on TACAN/DME on RO missions can be substantially penalizing. Therefore mitigation methods need to be applied. Time blanking, while effective for aircraft applications is here confirmed to be badly suited. For FDAF, where the residual C/N_0 degradation is still high, the Hybrid method is confirmed to perform best even though residual C/N_0 degradation is significant, due mostly to undetected pulses. This paper tackles first simulation results for space-born applications. Future works will cover specific parameters and detection method optimisation for each method presented here.

Moreover, deviation of real-world signals from the model used here will need additional efforts. In the future, other mission types may also be studied to determine the optimal jamming mitigation methods to properly use GPS L5 or GALILEO E5a/b signals at space orbits.

REFERENCES

- [1] C. Hegarty et al, "Methodology for Determining Compatibility of GPS L5 with existing systems and preliminary results", Proceedings of The Institute of Navigation Annual Meeting, Cambridge, MA, June 1999
- [2] F. Bastide, E. Chatre, C. Macabiau and B. Roturier, "GPS L5 and GALILEO E5a/E5b signal-to-noise density ratio degradation due to DME/TACAN signals: simulations and theoretical derivation", ION-NTM-2004.
- [3] M. Raimondi, C. Macabiau and O. Julien, « Frequency domain adaptative filtering against pulsed interference: performance analysis over Europe », ION NTM 2008
- [4] G. X Gao, "DME/TACAN Interference and its mitigation in L5/E5 bands", ION GNSS 2007
- [5] L. Musumeci and F. Dovis, "Use of the wavelet transform for interference detection and mitigation in GNSS", International Journal of Navigation and Observation, 2014
- [6] J. Li et al. "DME interference suppression algorithm based on signal separation estimation theory for civil aviation system", EURASIP Journal on wireless communications and networking, 2016
- [7] A. M. Wolff, D. Akos and S. Lo, "Potential radio frequency interference with the GPS L5 band for radio occultation measurements", Atmospheric Measurement Techniques, EGU, 2014
- [8] R. Onrubia et al. "DME/TACAN Impact Analysis on GNSS Reflectometry", *IEEE Journal of Selected Topics in Applied Earth Observations and Remote Sensing*, vol. 9, no. 10, pp. 4611-4620, Oct. 2016
- [9] "Aeronautical Telecommunications, Volume I, Radio Navigation Aids", Annex 10 to the convention on International Civil Aviation, ICAO/OACI.
- [10] B. Titus, J. Betz, C. Hegarty and R. Owen, « Intersystem and Intrasystem Interference Analysis Methodology », ION GNSS 2003, 9-12 september 2003, Portland.
- [11] T. Pratt and J. Owen, "BOC Modulation Waveforms", ION GNSS 2003, 9-12 september 2003, Portland
- [12] Report ITU-R M.2220, "Calculation method to determine aggregate interference parameters of pulsed RF systems operating in and near the bands 1164-1215 MHz and 1215-1300 MHz that may impact radionavigation-satellite service airborne and ground-based receivers operating in those frequency bands", 10/2011.